Complementary energy approach to contact problems based on consistent augmented Lagrangian formulation

Massimo Cuomo, Giulio Ventura

Complementary Energy Approach to Contact Problems Based on Consistent Augmented Lagrangian Formulation

M. CUOMO AND G. VENTURA
Istituto di Scienza delle Costruzioni, Facoltà di Ingegneria
University of Catania, V.le A. Doria 6, 95125, Catania, Italy

Abstract—A stress formulation for frictionless contact problems between deformable bodies is proposed. Linear compatibility equations are assumed, while the constitutive relations are supposed nonlinear, yet reversible, i.e., ruled by a convex strain potential. The relevant contact rules are formulated in terms of concave conjugated potentials, whose superdifferentials yield the constitutive laws for the unilateral contact interface. Generalization of the mixed Hellinger-Reissner functional, and of the functionals of total potential energy and of complementary energy are formulated. The last one is used for numerical developments. The functional is regularized by means of an augmented Lagrangian function. Solution to the saddle point problem arising from the regularization is obtained in the subspace of self-equilibrated stresses only, using equilibrium equations for condensing out the complementary stresses. In the paper, some examples of more complex unilateral contact relations are also presented.

Keywords—Complementary formulation, Contact, Augmented Lagrangian, Conjugate unilateral potentials.

1. INTRODUCTION

A general framework for the analysis of physical problems ruled by nonsmooth potentials is obtained by applying the tools of convex analysis and the notions of generalized differentials. The particularization to unilateral problems is a well-established matter, although computational problems are still open, especially when several types of nonlinearities are coupled together. The object of the paper is a formulation of contact problems that lend themselves to effective numerical implementation, that can be applied to geometric and material nonlinear problems. In this paper only unilateral contact without friction for structures with reversible (generally nonlinear) behaviour will be treated. In [1], the formulation was applied to no-tension materials, while extension to elasto-plastic problems was presented in [2].

In contact problems, a displacement formulation is usually adopted. A stress formulation appears useful when restrictions on the admissible values of the stresses are present, as in no-tension or no-compression materials. In these cases the solution, while unique in terms of stresses, can be undetermined in terms of displacements, since stress-free regions may exist. Another interesting field of applicability of stress based formulation appears to be multibody contact problems.

This study has therefore as its main goal the formulation of a generalized complementary energy functional for contact problems, derived from a mixed functional, and the development of a strategy of solution based on consistent discretization, which does not require the introduction of special equilibrated elements.

The present work has been partly sponsored by funds of MURST.

The solution of the numerical problem is obtained by introducing an augmented Lagrangian regularization of the nonsmooth ruling functional. This technique has first been introduced for contact problems by Simo [3], in an approximated form. In this paper we will present an exact form of the method, that has already been used in nonlinear mechanic problems [4,5]. Convergence results for the form of the regularization presented here are available in the literature.

2. STRUCTURAL MODEL

2.1. State Variables

The object of this paper is a contact problem between deformable bodies, when only small deformations are present, assuming a reversible material behaviour (eventually nonlinear, in the limit unilateral), and nonlinear boundary conditions, in the form of unilateral contact without friction. As indicated in Figure 1, B will denote the region occupied by the body, whose boundary ∂B is decomposed into three parts, ∂B_q, where surface tractions are applied, ∂B_u, where displacements are prescribed, and $\partial B_w \subseteq \partial B_q$, where contact can occur. Prescribed deformations and self stress fields will not be taken into account.

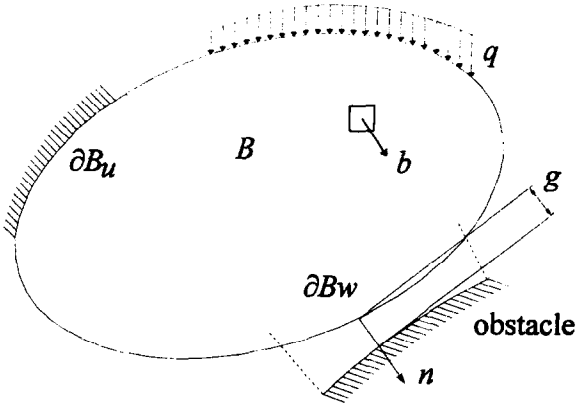

Figure 1. Definition of the body's boundaries.

The dual state variables u (displacements) and f (external forces) are elements of dual real linear vector spaces V and V'. For Cauchy's continuum, which we shall refer to in the sequel, it is

$$V = \{u \in (\mathcal{H}_1[B])^3,\ u = 0 \text{ on } \partial B_u\}.$$

Therefore, it is in general $u = u_0 + \hat{u}$, $u_0 \in V$, where $\hat{u}$ is a displacement function which satisfies nonhomogeneous boundary conditions.

For convenience, with the symbols $(v, v_\gamma, w, \hat{u})$ will be denoted displacements of points $\mathbf{x}$ in B, in $\frac{\partial B_q}{\partial B_u}$, in ∂B_w, and in ∂B_u, respectively. Similarly, the external forces f are partitioned as $f \equiv (b, q, p, r)$, b are volume forces, q are surface tractions on ∂Bq, p are the contact reactions, and r are the reactions on ∂B_u.

The duality pairing between V and V' will be denoted by $\langle\ ,\ \rangle_V$, then

$$\langle u, f\rangle_V = (v, b)_0 + \langle v_\gamma, q\rangle_{\partial V} + \langle w, p\rangle_{\partial V} + \langle u, r\rangle_{\partial V},$$

where $(\ ,\ )_0$ is the scalar product in L_2, and $\langle\ ,\ \rangle_{\partial V}$ denotes the duality pairing between $\mathcal{H}^{1/2}(\partial B)$ and $\mathcal{H}^{-1/2}(\partial B)$. In the case of Cauchy continuum, it is

$$\langle u, f\rangle_V = \int_B v \cdot b\, dB + \int_{\partial B_q} v \cdot q\, ds + \int_{\partial B_w} w \cdot p\, ds + \int_{\partial B_u} u \cdot r\, ds.$$

Similarly, the deformation ε and the internal forces σ are elements of dual linear vector spaces $\mathcal{D}, \mathcal{D}'$. In the case of continuous bodies, it is

$$\mathcal{D} = \{\varepsilon \in M_3\}, \qquad M_3 = \{\text{symmetric tensors on } R^3 \text{ whose elements} \in L_2\}.$$

The duality pairing between $\mathcal{D}, \mathcal{D}'$ is

$$\langle \varepsilon, \sigma \rangle_{\mathcal{D}} = \int_B \varepsilon * \sigma \, dB,$$

where $*$ stands for the scalar product between tensors.

2.2. The Equilibrium and Compatibility Relations

Linear compatibility equations are considered, indicated by a linear operator $C : V \to \mathcal{D}$, so that $Cu = \varepsilon$. The adjoint linear operator $C' : \mathcal{D}' \to V'$ yields the equilibrium conditions, $C'\sigma = f$.

In the case of Cauchy's continuum, it is

$$C = \text{sym grad}, \qquad C' = \begin{cases} -\,\text{div}, & \text{in } B, \\ P, & \text{on } \partial B_q, \end{cases}$$

where $P : \mathcal{D}' \to \mathcal{H}^{-1/2}(\partial B)$ is the mapping that yields the stress vector on the surface, i.e., $(P\sigma)_i = \sigma_{ij} n_j$.

2.3. The Material Constitutive Equations

Reversible material behaviour is considered, such that the constitutive map from $\mathcal{D}$ into $\mathcal{D}'$ can be obtained from a lower semicontinuous, convex strain potential $\phi(\varepsilon)$. The conjugate stress potential is defined by means of Legendre transform

$$\phi^c(\sigma) = \sup_{\varepsilon \in \mathcal{D}} [\langle \varepsilon, \sigma \rangle_{\mathcal{D}} - \phi(\varepsilon)].$$

In the applications, it has been assumed ϕ^c to be the linear elasticity stress potential, $\phi^c = (1/2)\langle E^{-1}\sigma, \sigma \rangle_{\mathcal{D}}$, but any nonlinear convex potential can be used, without any change in the algorithm that will be described.

2.4. Contact Conditions and the Force Potential

2.4.1. Local contact conditions

The displacement of a point P on ∂B_w at position x_P is limited by the presence of a certain number m of obstacles (Figure 2). If $h_i(x) \leq 0$ are the admissible regions ($h_i = 0$ are the equations of the surfaces of the obstacles), the unilateral contact laws are

$$h_i(x_P + w_P) \leq 0, \qquad i = 1, \ldots, m, \tag{1}$$

$$p(x_P) = p_{n_i} n_i, \qquad n_i = \frac{\nabla h_i(x_P)}{\|\nabla h_i(x_P)\|}, \qquad p_{n_i} \leq 0, \tag{2}$$

$$h_i(x_P + w_P) p_{n_i} = 0, \tag{3}$$

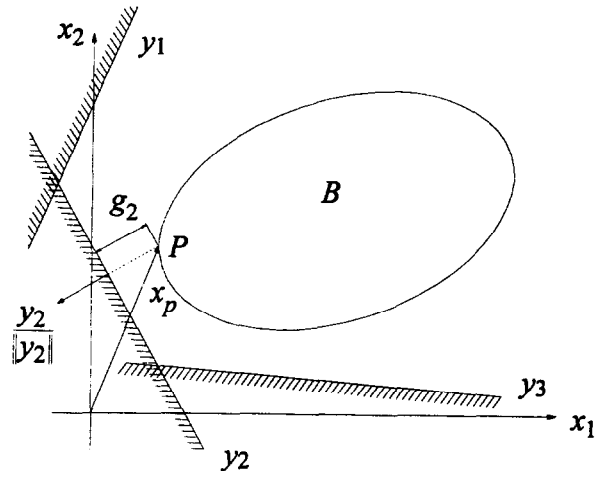

Figure 2. Multiple unilateral obstacles.

where n_i is the inward normal to the obstacle. Condition (2) holds for regular surfaces, such that the normal is uniquely defined in any point.

Let

$$W_i = \{w(x_P) : h_i(x_P + w_P) \leq 0\}, \qquad i = 1, \ldots, m.$$

Equation (1) can then be written as

$$w(x_P) \in W_n = \bigcap_{i=1}^{m} W_i.$$

Assuming that all W_i, and therefore their intersection, be convex sets, laws (1)–(3) show that w, p are dual variables, so the local contact constitutive equation can be written in the form

$$\begin{aligned} p(x_P) &\in \partial j(w_P), \\ w(x_P) &\in \partial j^c(p_P), \end{aligned} \tag{4}$$

where j, j^c are conjugate concave potentials of the unilateral constraint, defined as

$$j(w_P) = -\operatorname{ind} W_n, \tag{5}$$

$$j^c(p_P) = \inf_{w_P} [w_P \cdot p_P + \operatorname{ind} W_n]. \tag{6}$$

The symbol ∂ indicates the subdifferential set of a convex functional f, defined as (see [6])

$$\partial f(x) = \{x' \in X' : \langle x', y - x \rangle \leq f(y) - f(x)\}, \qquad \forall y \in X. \tag{7}$$

If the functional f is concave, then the symbol denotes the superdifferential, defined in the same way, provided that in equation (7) the $\leq$ sign is substituted by the $\geq$ sign.

Let h be an m-vector whose components are the m constraints h_i. From (4),(5) one has (see [7])

$$p_P \in \partial(-\operatorname{ind} W_n) = \partial(-\operatorname{ind}(R_-^m) \circ h)(x_P + w_P) = \partial(-\operatorname{ind}(R_-^m))[h(x_P + w_P)]\partial h(x_P + w_P), \tag{8}$$

where (R_-^m) is the cone of m-real vectors with nonpositive components. Equation (8) states that the contact reaction belongs to the normal cone at W_n in the point $x_P + w_P$. The last equality allows us to write

$$p_P \in \sum_{i=1}^{m} \lambda_i \partial h_i(x_P + w_P), \qquad \lambda_i \in \partial(-\operatorname{ind} R_-)[h_i(x_P + w_P)].$$

Therefore, at corner points of the admissible domain the total reaction is obtained as a conic combination of reactions normal to each of the constraint surfaces intersecting at that corner.

In order to derive an explicit expression for the conjugate potential j^c, the case of straight obstacles will be addressed, i.e., the constraint functions h_i are supposed to be linear, and will be written as

$$h_i(w_P) = y_i(x_P + w_P) - y_{o_i} \leq 0. \tag{9}$$

More explicitly, equation (9) can be rewritten as

$$w \cdot n_i \leq g_i, \qquad n_i = \frac{y_i}{\|y_i\|}, \qquad g_i = \frac{y_{o_i}}{\|y_i\|} - x_P \cdot n_i, \tag{10}$$

where, as before, n_i is the inward normal to the obstacle, and g_i represents the initial normal gap between point P and the i^{th} obstacle. The conjugate contact potential is evaluated first in the case of a single obstacle. We introduce the variable z such that its components along the normal and the tangent to the obstacle are $z_n = g - w_n$, $z_t = -w_t$; its domain of admissibility is the cone $Z_n = \{z : z_n \geq 0, \forall z_t\}$. Therefore one has

$$j^c(p) = \inf_w [w \cdot p + \operatorname{ind} W_n] = gp_n - \sup_z [z \cdot p - \operatorname{ind} Z_n] = gp_n - \operatorname{supp} Z_n = gp_n - \operatorname{ind} Z_n^0.$$

Here Z_n^0 is the polar cone to Z_n, and in this case $Z_n^0 = \{p : p_n \leq 0, p_t = 0\}$, and $p_n = p \cdot n$.

In the case of multiple obstacles, the support function can be evaluated observing that

$$\operatorname{ind} \bigcup_{i=1}^m W_{n_i} = \sum_{i=1}^m \operatorname{ind} W_{n_i}$$

and recalling that the conjugate of the finite sum of concave functions is their supremal convolution [7]. Then, the conjugate contact potential becomes

$$\begin{aligned} j^c(p_P) &= \inf_w \left[w \cdot p + \sum_{i=1}^m \operatorname{ind} W_{n_i} \right] = \sup_{p_i} \left[\sum_{i=1}^m (j_i^c(p_i)) \right]; \qquad \sum_{i=1}^m p_i = p, \\ &= \sup_{p_i} \left[\sum_{i=1}^m (-\operatorname{ind} Z_{n_i}^0 + g_i p_{n_i}) \right]; \qquad \sum_{i=1}^m p_{n_i} n_i = p, \\ &= -\operatorname{ind} Z_n^0 + \sum_{i=1}^m g_i p_{n_i}; \qquad \sum_{i=1}^m p_{n_i} n_i = p, \quad Z_n^0 = \sum_{i=1}^m Z_{n_i}^0. \end{aligned} \tag{11}$$

The level set at -1 of the functional (11) is the polar set to W_n, and turns out to be the convex hull of the polar sets to W_{n_i}.

Although the formulation of the problem will be quite general, the development of the numerical algorithm will refer to the simpler case of a single straight obstacle.

In the case of contact with a single obstacle, local contact relations simplify to

$$w \cdot n - g = w_n - g \leq 0, \qquad p \cdot n = p_n \leq 0, \qquad p_n(w_n - g) = 0. \tag{12}$$

The dual variables w_n and p_n are related by nonsmooth, concave potentials of the contact displacements,

$$p_n \in \partial j_n(w_n), \qquad w_n \in \partial j_n^c(p_n), \tag{13}$$

defined as

$$\begin{gathered} j_n(w_n) = -\operatorname{ind} W_n, \qquad W_n = \{w_n : w_n - g \leq 0\}, \\ j_n^c(p_n) = \inf_{w_n} \{p_n w_n + \operatorname{ind} W_n\} = \inf_{w_n \in W_n} p_n w_n = p_n g - \operatorname{ind} P_n, \\ P_n = \{p_n : p_n \leq 0\}. \end{gathered} \tag{14}$$

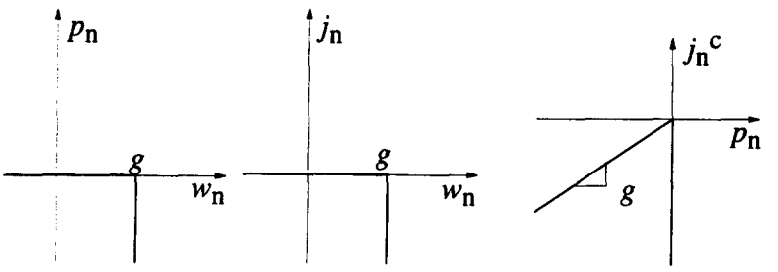

Figure 3. Constitutive equation, displacement and reactions potential for unilateral supports.

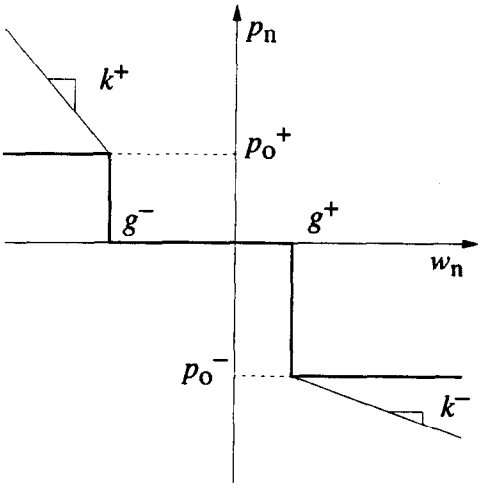

Figure 4. Generalized constitutive equation for unilateral supports.

Figure 3 illustrates the contact unilateral law and the conjugated potentials in this special case. From (14), we obtain the potential $j(w) : \mathcal{H}^{1/2}(\partial B_w) \to R$:

$$\begin{aligned} j(w) &= (j_n \cdot N)(w), \\ p \in \partial j(w) &= N^\top \partial j_n(Nw) = N^\top p_n, \\ j^c(p) &= \inf_w [w \cdot p - (j_n \cdot N)w] = (j_n^c \cdot N)p. \end{aligned} \tag{15}$$

In the last expression for j_n^c, there appears the indicator function of the set P_n, which is $P_n = \{p \in \mathcal{H}^{-1/2}(\partial B_w) : p_n \leq 0,\ p_t = 0\}$. N is the projector operator onto the normal to the contact surface.

2.4.2. Generalized unilateral contact conditions

Equations (14),(15) can be easily generalized to more complex contact constitutive laws, provided they are reversible. In such a case, in fact, it is always possible to obtain (nondifferentiable) potentials from the multivalued map $p_n = U(w_n)$, $U : \mathcal{H}^{1/2} \to \mathcal{H}^{-1/2}$.

As an example, the case shown in Figure 4 is examined. It models a type of constraint which limits the possible displacement of a point (e.g., a roller for a bridge span, provided with two security stops against excessive displacements due to seismic effects). Therefore, if $w_n \in]g^-, g^+[$, $p_n = 0$. When the displacement attains one of the limits, the reaction of the containing wall can grow (or decrease) up to a limit value p_0^+ (respectively, p_0^-), and then further displacements are allowed, either with constant or with linearly growing reaction. The constitutive law of the

constraint is then a composite map

$$
\begin{aligned}
&w_n < g^-, && p_n = p_0^+, && [p_n = k^+(w_n - g^-) + p_0^+,\ k^+ < 0],\\
&w_n = g^-, && p_n \in [0, p_0^+],\\
&w_n \in \,]g^-, g^+[\,, && p_n = 0,\\
&w_n = g^+, && p_n \in [p_0^-, 0],\\
&w_n > g^-, && p_n = p_0^-, && [p_n = k^-(w_n - g^+) + p_0^-,\ k^- < 0].
\end{aligned}
$$

The concave potential can be obtained as

$$
j_n(w_n) = \sup_{i=1,2,3} j_{n_i}(w_n),
$$

where j_{n_i} are the displacement potentials

$$
\begin{aligned}
j_{n_1}(w_n) &= p_0^+(w_n - g^-) - \operatorname{ind} W_{n_1}, \quad W_{n_1} = \{w_n : w_n - g^- < 0\},\\
&\left[k^+ \frac{(w_n - g^-)^2}{2} + p_0^+(w_n - g^-) - \operatorname{ind} W_{n_1}\right],\\
j_{n_2}(w_n) &= -\operatorname{ind} W_{n_2}, \quad W_{n_2} = \{w_n : w_n \in [g^-, g^+]\},\\
j_{n_3}(w_n) &= p_0^-(w_n - g^+) - \operatorname{ind} W_{n_3}, \quad W_{n_3} = \{w_n : w_n - g^+ > 0\},\\
&\left[k^- \frac{(w_n - g^+)^2}{2} + p_0^-(w_n - g^+) - \operatorname{ind} W_{n_3}\right].
\end{aligned}
$$

The graphs of j_{n_i} are presented in Figure 5. The concave hull of such graphs is the graph of j_n. The conjugate potential is then given by (see Figure 6):

$$
j_n^c(p_n) = \inf\left[w_n p_n - \sup_i j_{n_i}(w_n)\right] = \inf_i j_{n_i}^c(p_n),
$$

where simple calculations yield

$$
\begin{aligned}
j_{n_1}^c(p_n) &= p_n g^- - \operatorname{ind} P_{n_1}, \quad P_{n_1} = \{p_n : p_n < p_0^+\},\\
&\left[p_n g^- + \frac{1}{k^+}\frac{(p_n - p_0^+)_+^2}{2}\right], \quad (\,)_+ = \begin{cases} (\,), & \text{if } (\,) > 0,\\ 0, & \text{if } (\,) \le 0,\end{cases}\\
j_{n_2}^c(p_n) &= \begin{cases} p_n g^-, & \text{if } p_n > 0,\\ p_n g^+, & \text{if } p_n \le 0,\end{cases}\\
j_{n_3}^c(p_n) &= p_n g^+ - \operatorname{ind} P_{n_3}, \quad P_{n_3} = \{p_n : p_n > p_0^-\},\\
&\left[p_n g^+ + \frac{1}{k^-}\frac{(p_n - p_0^-)_+^2}{2}\right].
\end{aligned}
$$

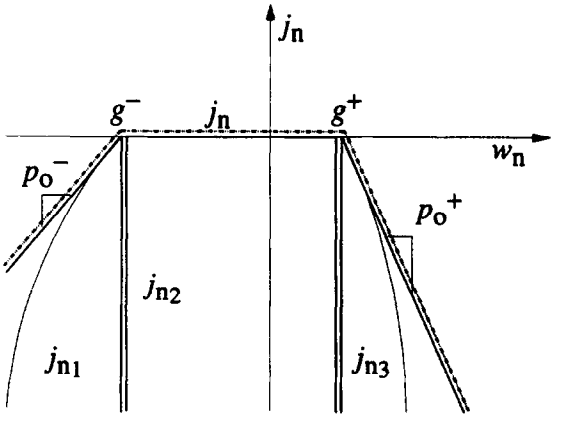

Figure 5. Generalized displacements potential for unilateral supports.

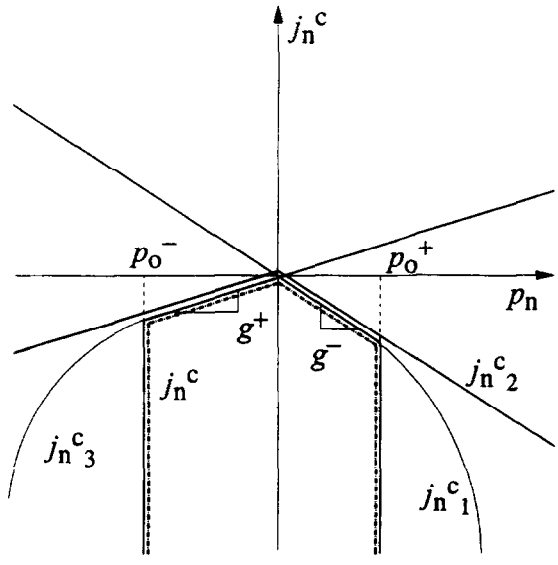

Figure 6. Generalized reactions potential for unilateral supports.

2.4.3. The force potential

The bilateral boundary conditions $u = \hat{u}$, $r \neq 0$, $r(u - \hat{u}) = 0$ on ∂B_i, can also be obtained from conjugate concave potentials

$$\begin{aligned} j_b(u) &= -\operatorname{ind}\{u - \hat{u}\}, \qquad & r \in \partial j_b(u), \\ j_b^c(r) &= \langle \hat{u}, r \rangle_{\partial V}, & u \in \partial j_b^c(r) = \hat{u}, \end{aligned}$$

illustrated in Figure 7. The global potentials of unilateral and bilateral constraints will be indicated with capital letters, e.g.,

$$\begin{aligned} J_n(w) &= -\operatorname{ind} \hat{W}_n, & \hat{W}_n &= \{w \in V : w_n(x) - g(x) \leq 0,\ \forall x\}, \\ J_n^c(p) &= \langle g(x), p_n(x) \rangle - \operatorname{ind} \hat{P}_n, & \hat{P}_n &= \{p \in V' : p_n(x) \leq 0,\ p_t(x) = 0,\ \forall x\}. \end{aligned} \tag{16}$$

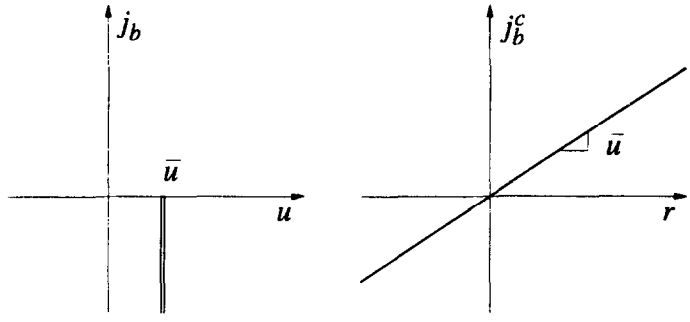

Figure 7. Displacements and reactions potentials for bilateral supports.

The global concave force and displacement potentials $\psi(u) : V \to R$, $\psi^c(f) : V' \to R$ take finally the following forms:

$$\begin{aligned} \psi(u) &= (v, b)_o + \langle v_\gamma, q \rangle_{\partial V} + J_n(w) + J_b(u), \\ \psi^c(f) &= \inf_{u \in V} [\langle u, f \rangle_V - \psi(u)] \\ &= \inf_{u \in V} [\langle w, p \rangle_{\partial V} + \langle u, r \rangle_{\partial V} - J_n(w) - J_b(u)] \\ &= J_n^c(p) + J_b^c(r) = \int_{\partial B_u} \hat{u} \cdot r \, ds + \int_{\partial B_w} p_n g \, ds - \operatorname{ind} \hat{P}_n. \end{aligned} \tag{17}$$

3. VARIATIONAL FORMULATION OF THE PROBLEM

The structural problem described in the previous section is a generalized elasticity problem, since it is ruled by convex or concave potentials. Therefore, the solution is characterized by the saddle point of the generalized Hellinger-Reissner functional, given by (see [8])

$$\begin{aligned}\Pi_R(\sigma,u) = -\phi^c(\sigma) - \psi(u) + \langle \sigma, Cu\rangle_{\mathcal{D}} = -\phi^c(\sigma) + \int_B Cu * \sigma \, dB \\ - \int_B v\cdot b\, dB - \int_{\partial B_q} v\cdot q\, ds + \operatorname{ind}\hat{W}_n + \operatorname{ind}\{u-\hat{u}\},\end{aligned} \tag{18}$$

concave in σ and convex in u. The variation of Π_R with respect to the displacement u yields the weak form of the equilibrium equations

$$0 \in \partial_u \Pi_R(\sigma,u) \Leftrightarrow 0 \in \partial\psi(u) - C'\sigma. \tag{19}$$

Applying Green's formula to (18), one has

$$\begin{aligned}\Pi_R(\sigma,u) = -\phi^c(\sigma) + \int_B \operatorname{div}\sigma\cdot u\, dB + \int_{\partial B} \sigma_n\cdot u\, ds - \int_B v\cdot b\, dB \\ - \int_{\partial B_q} v\cdot q\, ds + \operatorname{ind} W_n + \operatorname{ind}\{u-\hat{u}\}.\end{aligned}$$

Therefore, the equilibrium equations are explicitly written as

$$\begin{aligned}&\operatorname{div}\sigma = b, && \text{in } B,\\ &\sigma n = q, && \text{on } \frac{\partial B_q}{\partial B_u},\\ &\sigma n = p+q, && \text{on } \partial B_w,\\ &\sigma n = r, && \text{on } \partial B_u.\end{aligned} \tag{20}$$

3.1. Generalized Complementary Energy Functional

Extremization of the mixed functional (18) w.r.t. displacements gives

$$\begin{aligned}\inf_{u\in V}\Pi_R &= -\phi^c(\sigma) + \inf_{u\in V}[\langle\sigma, Cu\rangle_{\mathcal{D}} - \psi(u)]\\ &= -\phi^c(\sigma) + \inf_{u\in V}[\langle f,u\rangle_V - \psi(u) - \langle f,u\rangle_V + \langle\sigma,Cu\rangle_{\mathcal{D}}]\\ &= -\phi^c(\sigma) + \psi^c(f) + \inf_{u\in V}[\langle\sigma,Cu\rangle_{\mathcal{D}} - \langle f,u\rangle_V].\end{aligned}$$

The infimum of the term in the square brackets yields the equilibrium equations (20). The generalized form of the complementary energy principle is then obtained as

$$\Pi_c(\sigma,f) = -\phi^c(\sigma) + \psi^c(f), \qquad \forall\sigma\in\mathcal{D}' : C'\sigma = f, \tag{21}$$

that is concave in σ, f. It has to be noted that the unknown contact reactions p are related to the stresses through the equilibrium equations (20). The solution σ^* to the elastic problem is therefore given by

$$\sigma^* = \arg\sup_{\sigma\in\mathcal{D}'}\Pi_c(\sigma), \qquad \text{subject to } C'\sigma = f.$$

The explicit representation of the functional Π_c is

$$\Pi_c(\sigma) = -\frac{1}{2}\int_B E^{-1}\sigma\cdot\sigma\, dB + \int_{\partial B_u}\sigma n\cdot\hat{u}\, ds + \int_{\partial B_w} g p_n\, ds - \operatorname{ind}\hat{P}_n, \tag{22}$$

where for simplicity the linear elastic stress potential has been introduced.

An unconstrained formulation is obtained by decomposing the stress as $\sigma = \sigma_0 + \sigma_1$, so that $\sigma_0 \in \ker C'$, $\sigma_1 \in \Sigma_1$, where $\Sigma_1 = \{\sigma\in\mathcal{D}' : C'\sigma = f\}$. Substituting these in (22) turns Π_c into an unconstrained functional of σ_0 only, $\Pi_c(\sigma(\sigma_0))$.

3.2. Generalized Potential Energy Functional

Extremization of the mixed form (18) with respect to the stress components leads to the generalized total potential energy functional Π_e, dual to Π_c

$$\Pi_e(u) = \sup_{\sigma \in \mathcal{D}'} [-\phi^c(\sigma) + \langle \sigma, Cu \rangle_{\mathcal{D}}] - \psi(u) = \phi(Cu) - \psi(u), \qquad \forall u \in V. \tag{23}$$

The explicit expression of (23) in the case of linear elastic material is

$$\Pi_e(u) = \frac{1}{2} \int_B ECu \cdot Cu \, dB - \int_B b \cdot u \, dB - \int_{\partial B_q} q \cdot u \, ds - \operatorname{ind} \hat{W}_n(w), \qquad u = \hat{u} \text{ on } \partial B_u. \tag{24}$$

The functional Π_e is convex in u, and the solution u^*, provided it exists, is characterized by

$$u^* = \arg \min_{u \in V} \Pi_e(u).$$

3.3. Regularization of the Functionals

Functionals Π_c, Π_e are nondifferentiable because of the presence of the indicator functions. Several methods of regularization have been proposed; the ones widely used for numerical implementation of structural problems have been penalty, Lagrangian, and augmented Lagrangian methods. Lagrange methods lead to linear or nonlinear complementarity problems, solved by means of linear or nonlinear programming. Although often employed in the first formulations of contact problems [9–11], they are not very convenient from a computational point of view. Penalty methods, introduced by Fiacco and McCormick for constrained optimization [12], seem particularly well suited for the problem at hand, since the tangent stiffness matrix that rules the iterative problem (in the displacement formulation) is very simple, being the sum of the elastic stiffness matrix and a diagonal matrix of fictitious "stiff" contact spring constants. Usually external quadratic penalty functions have been used, although other penalty functionals, particularly of the interior type, can be employed. In [13], it has been shown that these alternative formulations can offer some advantages in specific problems (especially when interpenetration needs to be accurately avoided, as in multibody contact-impact problems). However, it is well known that penalty methods suffer from slow or poor convergence, especially when the penalty parameter becomes large, since the Hessian of the potential energy functional is not continuous. Therefore, attention turned toward perturbed [14] and augmented Lagrangian methods [3,4,15,16]. Augmented Lagrangian techniques, introduced by Hestenes and Powell [17,18] for constrained optimization problems, avoid the difficulties with penalty methods, since there is no diverging parameter, and also those with classical Lagrangian methods, since the evaluation of the Lagrange multipliers is equivalent to the optimization of a dual functional, convex with respect to the multipliers. In [4,16], a comparison between Lagrangian and augmented Lagrangian algorithms for contact problems is shown, while in [3,5], numerical approximations of augmented Lagrangian formulation are compared with the analogous penalty formulations.

Details of the implementation of the method will be given in the following sections. It is based on the following result relative to indicator functions:

$$K = \{x \in X : h(x) = 0, \; h : X \to R\},$$
$$\operatorname{ind} K(x) = \sup_{\lambda \in R} \left(\lambda h(x) + \frac{1}{2} \alpha h^2(x) \right), \qquad \alpha \in R_+.$$

The term in parentheses is named augmented Lagrangian function $\mathcal{L}$. The equal sign holds only for equality constraints. For inequality constraints, i.e., $h(x) \leq 0$, the correct expression is

obtained by defining a new equality constraint $\bar{h}(x) = \inf_{z\geq 0}(h(x)+z) = 0$, using slack variables z (see [19]). Then one has

$$\mathcal{L}(x,\lambda,z) = \lambda\bar{h}(x) + \frac{1}{2}\alpha\bar{h}^2(x) = \inf_{z\geq 0}\left(\lambda(h(x)+z) + \frac{1}{2}\alpha(h(x)+z)^2\right). \tag{25}$$

The value of z that yields the infimum can be explicitly calculated from the gradient of the previous expression, thus

$$\nabla_z\mathcal{L} = \lambda + \alpha(h(x)+z) = 0, \qquad z = \max\left(0, -\frac{\lambda}{\alpha} - h(x)\right).$$

Therefore one has

$$\bar{h}(x) = h(x) + \max\left(0, -\frac{\lambda}{\alpha} - h(x)\right) = \max\left(h(x), -\frac{\lambda}{\alpha}\right). \tag{26}$$

It has to be noted that the transformation of the inequality constraint $h(x) \leq 0$ into an equality one could also be obtained by means of Macauley bracket

$$h(x) \leq 0 \Leftrightarrow (h)_+ = 0, \qquad \mathcal{L}_M = \lambda(h)_+ + \frac{1}{2}\alpha(h)_+^2. \tag{27}$$

This approach has been used in an augmented Lagrangian scheme by some authors [3,16]. Between the two formulations there exist remarkable differences. A plot of $\mathcal{L}, \mathcal{L}_M$ is presented in Figure 8, compared with penalty regularization. The two augmented Lagrangian functions are both continuous at the origin, but $\mathcal{L}_M$ has zero first derivative, while $\mathcal{L}$ has a slope equal to λ. Moreover, Figure 9 shows that $\mathcal{L}_M$ has discontinuous second derivative at the origin, precluding the extension of the theoretical results known for the equality constraint case (based on the continuity of the Hessian of the augmented Lagrangian functional in a neighbourhood of the solution) and degrading the convergence properties of the numerical algorithms.

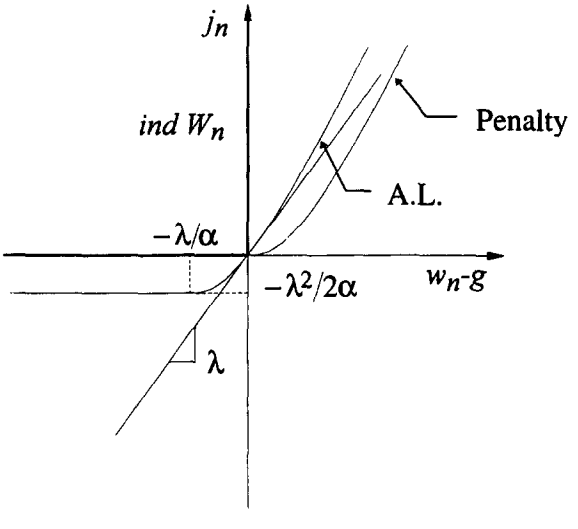

Figure 8. Regularizations of the indicator function of the admissible domain via Lagrangian, augmented Lagrangian, and penalty approximations.

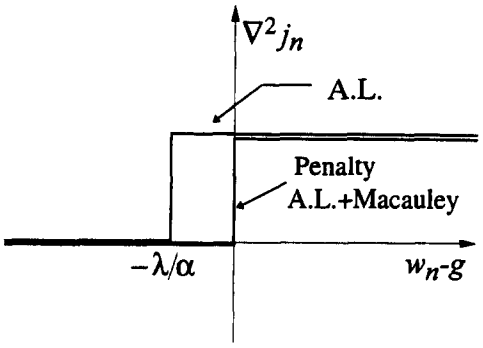

Figure 9. Second derivative of the augmented Lagrangian function compared with the second derivative of penalty and augmented Lagrangian with Macauley bracket function.

Introducing the regularization (25) in the functionals Π_c, Π_e, (22), (24), two dual mixed functionals are obtained,

$$\Pi_c^{al} = -\frac{1}{2}\int_B E^{-1}\sigma\cdot\sigma\, dB + \int_{\partial B_u} \sigma n\cdot\hat{u}\, ds + \int_{\partial B_w} g p_n\, ds + \int_{\partial B_w}\left(\mu\bar{p}_n - \frac{1}{2}\alpha\bar{p}_n^2\right) ds, \qquad \bar{p}_n = \max\left(p_n, \frac{\mu}{\alpha}\right), \tag{28}$$

$$\Pi_e^{al} = \frac{1}{2}\int_B ECu\cdot Cu\, dB - \int_B b\cdot u\, dB - \int_{\partial B_q} q\cdot u\, ds - \int_{\partial B_w}\left(\gamma(\overline{w_n-g}) + \frac{1}{2}\beta(\overline{w_n-g})^2\right) ds, \qquad \overline{w_n-g} = \max\left(w_n-g, -\frac{\gamma}{\beta}\right). \tag{29}$$

Note that in (28) the sign of the Lagrangian multiplier has been changed and $(-\sup\mathcal{L}(\mu,p_n))$ has been turned into $(\inf -\mathcal{L}(\mu,p_n))$. In these augmented functionals, μ,γ have the meaning of contact displacement $w_n - g$ and of contact reaction $-p_n$, respectively. Consequently, α,β represent compliance and stiffness constants of fictitious springs active when interpenetration occurs. The solution is obtained as saddle point of the problems

$$\inf_{\mu}\sup_{\sigma,p_n}\Pi_c^{al}(\sigma,\mu), \qquad \sup_{\gamma}\inf_{u\in V}\Pi_e^{al}(u,\gamma).$$

Note that in the algorithm, Lagrangian multipliers are unconstrained variables.

4. DISCRETIZED FORMULATION OF THE COMPLEMENTARY ENERGY FUNCTIONAL

4.1. Nodal Variables

A solution method based on the generalized complementary energy functional will now be described.

Although it is not strictly necessary, both stress and displacement fields are separately discretized on a FE mesh

$$\sigma = G_\sigma \mathbf{s}, \qquad u = G_u \mathbf{u}. \tag{30}$$

Discretization of displacements is necessary only for their numerical calculation, once the solution in terms of stresses has been achieved. However, it will be used directly in the Hellinger-Reissner functional in order to obtain discretized equilibrium equations in a consistent way.

Discretization of the contact variables can be performed either by introducing special contact elements where displacements or reactions can be interpolated, or by using the same discretization as for the bulk variables. We denote by $\mathbf{w}$ the nodal displacement of nodes belonging to the

contact boundary, $\mathbf{v}$ the remaining ones, and $\mathbf{n}(s)$ the inward normal to the obstacle. Then the normal contact displacement w_n in discretized form becomes

$$w_n = G_u(s)\mathbf{w} \cdot \mathbf{n}(s) = NG_u(s)\mathbf{w}. \tag{31}$$

Discretized contact reactions are obtained from the expression for the virtual work,

$$\int_{\partial B_w} p_n(s)(NG_u(s)\mathbf{w})\, ds = \int_{\partial B_w} G_u^\top(s) N^\top p_n\, ds\, \mathbf{w} = \mathbf{p} \cdot \mathbf{w}. \tag{32}$$

In this way, only nodal reactions can be directly evaluated, while their distribution over the boundary is undetermined. In discretized form, the contact potentials become

$$\psi(G_u\mathbf{v}) = \int_B G_u^\top b\mathbf{v}\, dB + \int_{\partial B_q} G_u^\top q\mathbf{v}\, ds - \operatorname{ind}\hat{W}_n(NG_u\mathbf{w}) = \mathbf{f} \cdot \mathbf{v} - \operatorname{ind}\hat{W}_n(NG_u\mathbf{w}), \tag{33}$$

$$\begin{aligned}\psi_c(f) &= \inf_{\mathbf{v},\mathbf{w}} \left\{ \mathbf{v} \cdot \mathbf{f} + \mathbf{w} \cdot \mathbf{p} - \mathbf{v} \cdot \mathbf{f} + \operatorname{ind}\hat{W}_n(NG_u\mathbf{w}) \right\} \\ &= \int_{\partial B_w} p_n(s) g(s)\, ds - \operatorname{ind}\hat{P}_n. \end{aligned} \tag{34}$$

The last expression is easily evaluated in the case of a single obstacle. Recalling expression (10) for g, and using isoparametric interpolation for the nodal coordinates, the first term of ψ_c becomes

$$\int_{\partial B_w} p_n(s) g(s)\, ds = \int_{\partial B_w} p_n(s) G_u(s)\mathbf{x} \cdot \mathbf{n} \left(\frac{y_o}{\mathbf{y} \cdot \mathbf{x}} - 1 \right) ds = \mathbf{p} \cdot \mathbf{g}, \quad g_i = \frac{y_o}{\|\mathbf{y}\|} - \frac{\mathbf{x}_i \cdot \mathbf{y}}{\|\mathbf{y}\|}. \tag{35}$$

The components of $\mathbf{g}$ have the meaning of nodal values of the gap function, and are interpolated by the shape functions adopted for the contact displacements as suggested in general cases [20].

The discretized form of the dual force potential becomes then

$$\psi_c(\mathbf{p}) = \mathbf{p} \cdot \mathbf{g} - \operatorname{ind} P_{n_h}, \tag{36}$$

where the set P_{n_h} is a discretized form of the set $\hat{P}_n$ [21]

$$P_{n_h} = \{\mathbf{p} : p_{n_i} \leq 0,\ p_{t_i} = 0,\ \forall \text{ nodes } i \in \partial B_w\}.$$

4.2. Equilibrium Equations Discretized

The weak form of the equilibrium equations obtained from the variation of (18) is

$$\langle \sigma, C\tilde{u} \rangle_{\mathcal{D}} - (b, \tilde{u})_0 - \langle q, \tilde{u} \rangle_{\partial V} - j(u_n + \tilde{u}_n) + j(u_n) \geq 0, \qquad \forall\, \tilde{u},$$

that is,

$$\langle \sigma, C\tilde{u} \rangle_{\mathcal{D}} - (b, \tilde{u})_0 - \langle q, \tilde{u} \rangle_{\partial V} = \langle p_n, \tilde{u}_n \rangle, \qquad p_n \in \partial j_n(w_n). \tag{37}$$

Inserting in (18) the discretization (30) of σ, u, one has

$$\begin{aligned}
\int_B (CG_u)^\top G_\sigma\, dB\, \mathbf{s} \cdot \mathbf{v} &= \int_B G_u^\top b\, dB \cdot \mathbf{v} + \int_{\partial B_q} G_u^\top q\, ds \cdot \mathbf{v}, \\
\int_B (CG_u)^\top G_\sigma\, dB\, \mathbf{s} \cdot \mathbf{w} &= \int_{\partial B_w} G_u^\top q\, ds \cdot \mathbf{w} + \int_{\partial B_w} G_u^\top N^\top p_n\, ds \cdot \mathbf{w}, \\
\int_B (CG_u)^\top G_\sigma\, dB\, \mathbf{s} \cdot \mathbf{u} &= \int_{\partial B_u} G_u^\top r\, ds \cdot \mathbf{u},
\end{aligned}$$

where the first set of equations refer to internal nodes, the second to nodes on ∂B_w, and the third to nodes on ∂B_u. The equations are set as

$$\begin{bmatrix} \mathbf{C} \\ \mathbf{Q} \\ \mathbf{H} \end{bmatrix} [\mathbf{s}] = \begin{bmatrix} \mathbf{f} \\ \mathbf{q} \\ \mathbf{r} \end{bmatrix} + \begin{bmatrix} \mathbf{0} \\ \mathbf{p} \\ \mathbf{0} \end{bmatrix}, \tag{38}$$

where $\mathbf{C} : R^\tau \to R^{n-l}$, $\mathbf{Q} : R^\tau \to R^l$, $\mathbf{H} : R^\tau \to R^c$ (n = number of free nodal displacements, l = number of contact nodes, c = number of assigned displacements, τ = dimension of the space of the stress components).

The stress variables are partitioned in the set of the self-equilibrated stresses $\mathbf{s}_0$, of dimension $\tau - n + l$, and the set of the stresses in equilibrium with the external forces, $\mathbf{s}_1$, of dimension $n - l$. The equilibrium equations are then written as

$$\begin{bmatrix} \mathbf{C}_0 & \mathbf{C}_1 \\ \mathbf{Q}_0 & \mathbf{Q}_1 \\ \mathbf{H}_0 & \mathbf{H}_1 \end{bmatrix} \begin{bmatrix} \mathbf{s}_0 \\ \mathbf{s}_1 \end{bmatrix} = \begin{bmatrix} \mathbf{f} \\ \mathbf{q} \\ \mathbf{r} \end{bmatrix} + \begin{bmatrix} \mathbf{0} \\ \mathbf{p} \\ \mathbf{0} \end{bmatrix}. \tag{39}$$

The partition of the stresses must be performed in such a way that the submatrix $\mathbf{C}_1$ be invertible. In practice, this is accomplished by a Gaussian reduction. The equilibrated stresses $\mathbf{s}_1$ and the contact reactions $\mathbf{p}$ can be obtained explicitly solving equations (39) with respect to the self-equilibrated stresses $\mathbf{s}_0$

$$\mathbf{s}_1 = -\mathbf{C}_1^{-1}\mathbf{C}_0\mathbf{s}_0 + \mathbf{C}_1^{-1}\mathbf{f}. \tag{40}$$

The solution of (39) becomes

$$\mathbf{s} = \begin{bmatrix} \mathbf{s}_0 \\ \mathbf{s}_1 \end{bmatrix} = \mathbf{R}\mathbf{s}_0 + \mathbf{t}, \qquad \mathbf{R} = \begin{bmatrix} \mathbf{I} \\ -\mathbf{C}_1^{-1}\mathbf{C}_0 \end{bmatrix}, \qquad \mathbf{t} = \begin{bmatrix} \mathbf{0} \\ \mathbf{C}_1^{-1}\mathbf{f} \end{bmatrix}, \tag{41}$$

$$\mathbf{p} = \mathbf{Q}\mathbf{R}\mathbf{s}_0 + \mathbf{a}, \qquad \mathbf{Q}\mathbf{R} = \mathbf{Q}_0 - \mathbf{Q}_1\mathbf{C}_1^{-1}\mathbf{C}_0, \qquad \mathbf{a} = \mathbf{Q}\mathbf{t} - \mathbf{q} = \mathbf{Q}_1\mathbf{C}_1^{-1}\mathbf{f} - \mathbf{q}, \tag{42}$$

$$\mathbf{r} = \mathbf{H}\mathbf{R}\mathbf{s}_0 + \mathbf{b}, \qquad \mathbf{H}\mathbf{R} = \mathbf{H}_0 - \mathbf{H}_1\mathbf{C}_1^{-1}\mathbf{C}_0, \qquad \mathbf{b} = \mathbf{H}\mathbf{t} = \mathbf{H}_1\mathbf{C}_1^{-1}\mathbf{f}. \tag{43}$$

4.3. Discretization of Complementary Energy Functional

Using expressions (41)–(43) for enforcing equilibrium, and the augmented Lagrangian regularization (25), the expression (28) of Π_c^{al} takes the discretized form

$$\Pi_c^{al}(\mathbf{s}_0) = -\int_B \phi^c(G_\sigma(\mathbf{R}\mathbf{s}_0 + \mathbf{t}))\, dB + (\mathbf{H}\mathbf{R}\mathbf{s}_0 + \mathbf{b}) \cdot \hat{\mathbf{u}} + (\mathbf{Q}\mathbf{R}\mathbf{s}_0 + \mathbf{a}) \cdot \mathbf{g} + \mu \cdot \bar{\mathbf{p}} - \frac{1}{2}\alpha \sum_{i=1}^{l} \bar{p}_i^2, \tag{44}$$

where $\mu_i = w_{n_i} - g_i$, $\bar{p}_i = \max(p_i, \mu_i/\alpha)$. It has to be noted that in (44) the contact displacement variables μ are evaluated at nodal points, since they are directly interpolated.

In the special case of linear elastic behaviour, the functional (44) becomes, after some algebra,

$$\begin{aligned} \Pi_c^{al} &= -\frac{1}{2}\mathbf{R}^\top\mathbf{F}\mathbf{R}\mathbf{s}_0 \cdot \mathbf{s}_0 - \mathbf{R}^\top\mathbf{F}\mathbf{t} \cdot \mathbf{s}_0 + \mathbf{R}^\top\mathbf{H}^\top\hat{\mathbf{u}} \cdot \mathbf{s}_0 + \mathbf{R}^\top\mathbf{Q}^\top\mathbf{g} \cdot \mathbf{s}_0 \\ &\quad + \sum_{i=1}^{l} \left[\bar{p}_{n_i}(\mathbf{s}_0)\mu_i - \frac{1}{2}\alpha(\bar{p}_{n_i}(\mathbf{s}_0))^2\right], \\ \mathbf{F} &= \int_B G_\sigma^\top \nabla^2\phi_c(\sigma) G_\sigma \, dB, \end{aligned} \tag{45}$$

after eliminating inessential constant terms.

For a Newton-like method of minimization, the gradient and the Hessian of (45) have to be evaluated:

$$\nabla_{\mathbf{s}_0}\Pi_c^{al} = -\mathbf{R}^\top \int_B G_\sigma^\top \nabla\phi_c(\sigma(\mathbf{s}_0))\, dB + \mathbf{R}^\top\mathbf{H}^\top\hat{\mathbf{u}} + \mathbf{R}^\top\mathbf{Q}^\top\mathbf{g} + \nabla\mathcal{L}(\mathbf{s}_0), \tag{46}$$

$$\nabla\mathcal{L}(\mathbf{s}_0) = \mathbf{R}^\top\mathbf{Q}^\top(\check{\mu} + \alpha\check{p}), \quad \check{\mu} = \Delta\mu, \quad \check{p} = \Delta p, \quad \Delta_{ij} = \begin{cases} 0, & \text{if } p_i < \dfrac{\mu_i}{\alpha}, \\ \delta_{ij}, & \text{if } p_i \geq \dfrac{\mu_i}{\alpha}, \end{cases}$$

$$\nabla^2_{\mathbf{s}_0}\Pi_c^{al} = -\mathbf{R}^\top\mathbf{F}\mathbf{R} + \nabla^2\mathcal{L}(\mathbf{s}_0), \tag{47}$$

$$\nabla^2\mathcal{L}(\mathbf{s}_0) = \alpha\mathbf{R}^\top\mathbf{Q}^\top\Delta\mathbf{Q}\mathbf{R}.$$

The matrix Δ appearing in (46),(47) selects only active constraints in the construction of the gradient and the Hessian. The expression (46) of $\nabla\Pi_c^{al}$ is the discretized form of the compatibility equations rot rot $\varepsilon = 0$. Indeed, it can be rewritten as [2]

$$\mathbf{R}^\top\mathbf{e} - \mathbf{R}^\top\mathbf{H}^\top\hat{\mathbf{u}} - \mathbf{R}^\top\mathbf{Q}^\top\mathbf{w} = 0,$$

$\mathbf{e}$ being the discretized deformations, and the next two terms are deformations due to imposed displacements and to the displacements of contact nodes.

4.4. The Augmented Lagrangian Numerical Implementation

The saddle point problem for the augmented Lagrangian functional is solved performing the minimization on the direct variables and the maximization on the dual ones through two distinct iterations. Different numerical methods can be chosen for each one, as well as different augmented Lagrangian iteration schemes [22], like the "classical" iteration scheme in which first minimization on the direct variables is achieved and then one step of the dual iteration is done, or the "diagonal" scheme in which alternatively one step of the direct and one step of the dual iteration is performed, until the norm of the constraint function $\|\bar{p}\|$ is reduced sufficiently. In the present implementation, the iterative scheme proceeds through the alternate steps

$$\mathbf{s}_0^{(k)} = \arg\left[\sup_{\mathbf{s}_0}\Pi_c^{al}\left(\mathbf{s}_0, \lambda^{(k-1)}, \mu^{(k-1)}\right)\right]_\varepsilon, \qquad \mu^{(k)} = \mu^{(k-1)} - \alpha\bar{p}_n\left(\mathbf{s}_0^{(k)}\right), \tag{48}$$

in which the penalty parameters can be kept constant or incremented during the iterations. The symbol $[\,]_\varepsilon$ indicates minimum computed with gradient tolerance ε ($\|\nabla_{\mathbf{s}_0}\Pi_c^{al}\| \leq \varepsilon$).

The pure Newton method is used for the minimization in the stresses, while a first-order formula (corresponding to the application of a pure gradient method on the dual problem $\inf\Pi_c'(\mu, \sigma(\mu))$) is used for the Lagrangian multipliers update. It should be noted that the first-order formula is a local update formula, i.e., it involves only the evaluation of the constraint function at the point selected for the contact. On the contrary, second-order formulas, while exhibiting better convergence properties, involve at least the evaluation of the gradients of the constraints with respect to the whole direct variables set and the construction and solution of several large systems of linear equations. Some details on these aspects can be found in [22,23].

It should be noted, however, that in practical applications it is not possible to minimize exactly the functional with respect to the direct variables as required by the iteration scheme described above, and anyway a numerically accurate minimization is a hard computational task. Moreover, it is known that in order to ensure a fast enough convergence of the algorithm, the penalty parameters should be set to a value greater than a threshold value which is unknown *a priori*. To override these difficulties, the following incremental scheme for the penalty parameters has been suggested by various authors [19]:

$$\alpha^{(k+1)} = \begin{cases} \rho\alpha^{(k)}, & \text{if } |\bar{p}^{(k)}| > \delta|\bar{p}^{(k-1)}|, \\ \alpha^{(k)}, & \text{otherwise}, \end{cases} \tag{49}$$

where usually $\rho = 10.0$, $\delta = 0.25$. This incremental scheme ensures a good convergence rate for the Lagrange multipliers and has the property that if the sequence of the multipliers is bounded, then the sequence $\{\alpha^{(k)}\}$ is bounded, too.

Asymptotically exact optimization of the functional with respect to the direct variables can be achieved if the following stopping criterion for the minimization procedure is introduced:

$$\left|\nabla_{\mathbf{s}_0}\Pi_{al}^{(k)}\right| \leq \varepsilon_k,$$

where $\{\varepsilon_k\}$ is a nonincreasing sequence, $\varepsilon_k \geq 0$, $\varepsilon_k \to 0$, so that the minimization becomes more precise after each multiplier iteration and asymptotically exact [19]. A linear rate of convergence is obtained if the nonincreasing sequence $\{\varepsilon_k\}$ is replaced by the sequence $\min(\varepsilon_k, c_k\|h^{(k)}\|)$, $\{c_k\}$ being a nonincreasing sequence $0 < c_{k+1} < c_k$.

The convergence proof of this approach for the first-order formula has been given by Bertsekas in 1982 [19]. The algorithm can then be synthesized as follows.

First, a trial solution for the stresses is chosen. Linear elastic solution obtained by considering all constraints bilateral with imposed displacements equal to the gaps is used. Then the following steps are performed.

Step 1.

$$\text{Fix } \delta, \gamma, \alpha^0, \varepsilon_{\min}, \varepsilon_{\max}, \text{ tol.}$$

Step 2.

$$\varepsilon^{(k)} = \min\left\{\varepsilon_{\max}, \varepsilon^{(k-1)}, \frac{1}{\alpha^{(k-1)}}\|\bar{p}\|^2\right\},$$

$$\varepsilon_k = \max\{\varepsilon^{(k)}, \varepsilon_{\min}\}.$$

Step 3.

$$\mathbf{s}_0^{(k)} = \arg\left[\sup_{\mathbf{s}_0} \Pi_{al}\left(\mathbf{s}_0, \mu^{(k-1)}\right)\right]_{\varepsilon_k}.$$

Step 4.

$$\mu^{(k)} = \mu^{(k-1)} - \alpha^{(k)}\bar{p}_n\left(\mathbf{s}_0^{(k)}\right).$$

Step 5.

$$\text{If } \left\|\bar{p}_n^{(k)}\right\| > \delta\left\|\bar{p}_n^{(k-1)}\right\|, \qquad \text{then } \alpha^{(k+1)} = \rho\alpha^{(k)}.$$

Step 6. Convergence test:

$$\text{if } \|\bar{p}_n\| < \text{tol, then terminate the computation; else go to Step 2.}$$

In this algorithm, the employment of the penalty parameter increment scheme (Step 5) and the asymptotic convergence in the variables $\mathbf{s}_0$ enforced by the sequence ε_k (Step 2) guarantee an efficient and reliable computation of the saddle point.

4.5. Computation of the Nodal Displacements

The nodal displacements of the finite elements mesh can be obtained from the Euler-Lagrange equations of the extended Hellinger-Reissner functional. In fact, the variation with respect to the nodal stresses $\mathbf{s}$ gives the following discrete compatibility equations:

$$\mathbf{C}^\top\mathbf{u} = \mathbf{F}\mathbf{s} - \mathbf{H}^\top\bar{\mathbf{u}} - \mathbf{Q}^\top\mathbf{w} + \mathbf{Q}^\top\overline{\mathbf{w} - \mathbf{g}}. \tag{50}$$

Introducing the partition of the compatibility matrix as in (39), the equations (50) split into the following two:

$$\begin{aligned}\mathbf{C}_0^\top\mathbf{u} &= \mathbf{F}_0\mathbf{s} - \mathbf{H}_0^\top\bar{\mathbf{u}} - \mathbf{Q}_0^\top\mathbf{w} + \mathbf{Q}_0^\top\overline{\mathbf{w} - \mathbf{g}},\\ \mathbf{C}_1^\top\mathbf{u} &= \mathbf{F}_1\mathbf{s} - \mathbf{H}_1^\top\bar{\mathbf{u}} - \mathbf{Q}_1^\top\mathbf{w} + \mathbf{Q}_1^\top\overline{\mathbf{w} - \mathbf{g}},\end{aligned} \tag{51}$$

where the subscripts 0 or 1 refer to a partition of the matrices analogous to that used for $\mathbf{C}$.

Nodal displacements are computed from the second of (51), the matrix $\mathbf{C}_1$ being nonsingular. The first equation of (51) coincides with the compatibility condition $\nabla\Pi_c = 0$, as can be seen substituting the displacements $\mathbf{u}$ calculated from the other equation.

5. NUMERICAL EXAMPLES

The method presented has been applied to the engineering problem of Figure 10, relative to the internal shell of a deep tunnel, whose section is made by two circular arcs of radii 5.55 m and 10.60 m. The width is 11.10 m, the height 9.8 m, and the thickness is 0.60 m in the bottom part and 0.8 m in the upper part. The tunnel lies in a soil with a weight per unit volume of $20.6\,\mathrm{KN/m^3}$, a friction angle of 25°, and a cohesion of $24.5\,\mathrm{KN/m^2}$. The loading distribution has been determined using the classical Terzaghi theory. The objective of the application is to evaluate contact pressures, in order to improve Terzaghi's hypothesis.

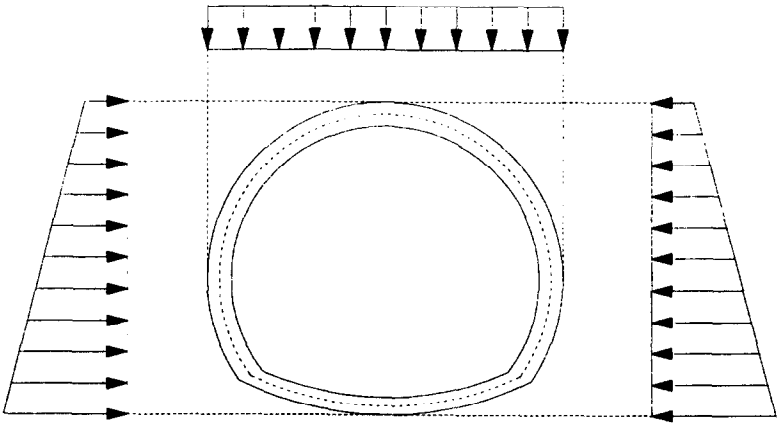

Figure 10. Tunnel section and loading.

The analysis has been carried out using four nodes linear isoparametric elements in plane strain, discretizing half of the structure, and considering unilateral frictionless supports along the whole boundary. The program starts its execution assuming as first trial solution the linear elastic solution computed considering all supports as bilateral and imposing boundary displacements equal to the gaps (zero in this example). The final solution is then found using the augmented Lagrangian iteration. The Signorini conditions were not violated during the iterations. The final diagrams of the bending moment and of the axial force are reported in Figure 11, while the maximum and minimum principal stresses are plotted in Figure 12.

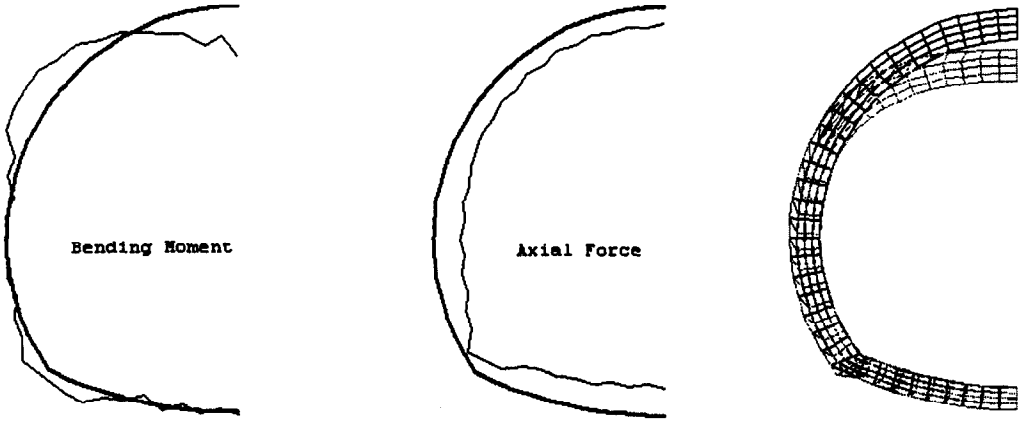

Figure 11. Bending moment, axial force, and displacements for the structure of Figure 10.

The second example is the classical Hertz problem of a circular semicylinder of infinite length pushed against a rigid plane obstacle. This simple example has been used for showing the type of convergence exhibited by the method. The problem has been analyzed starting from the linear elastic solution with supports displacements equal to the gaps. The solution has been sought

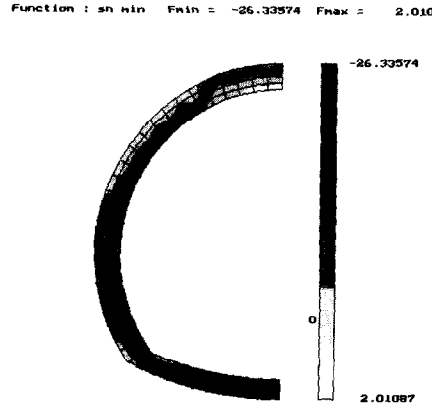

Function: sn min, Fmin = −26.33574, Fmax = 2.01087.

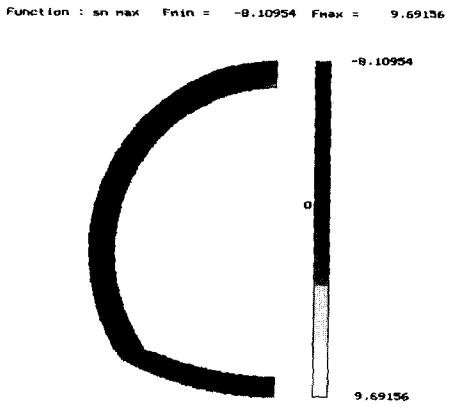

Function: sn max, Fmin = −8.10954, Fmax = 9.69156.

Figure 12. Maximum and minimum principal stresses for the structure of Figure 10.

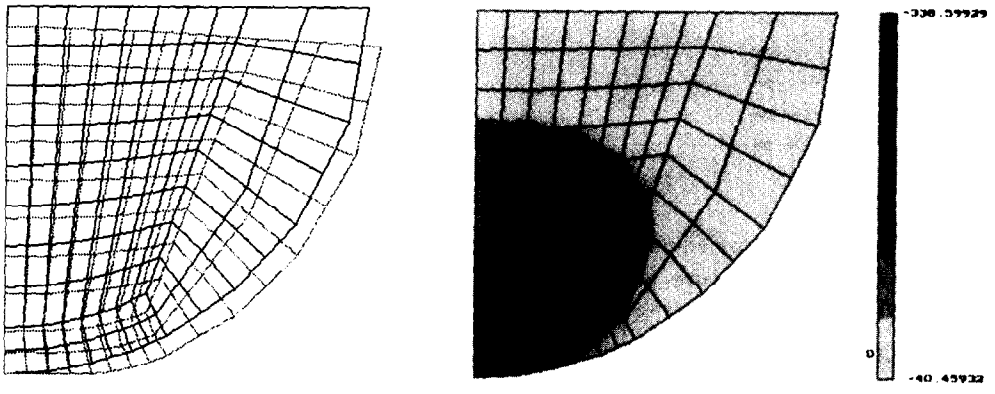

Figure 13. Final displacements and minimum principal stress for the Hertz problem.

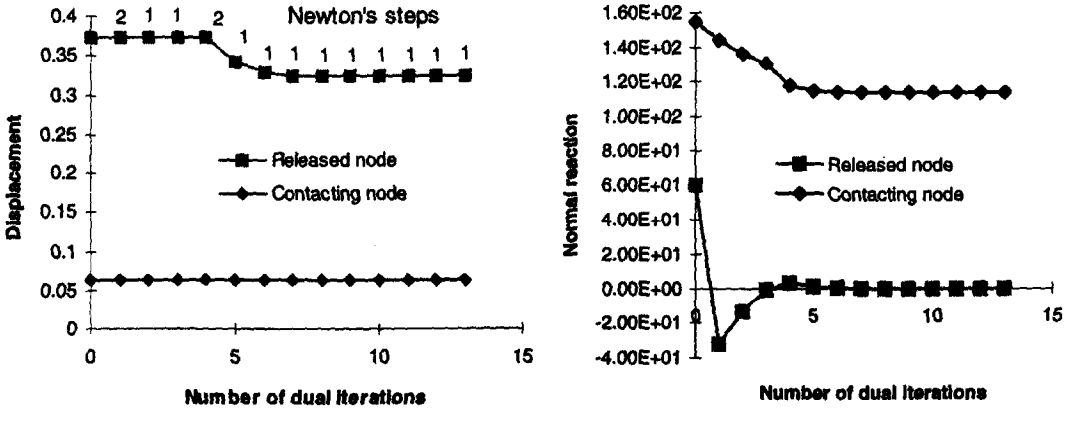

Figure 14. Convergence for displacements and reactions of two nodes in the Hertz problem.

using a very low initial penalty parameter (0.001), in order to slow down convergence and to show the typical behavior of the numerical algorithm.

In the graphs of Figures 13 and 14, two nodes unilaterally constrained have been considered. The first remains in contact also in the final solution, while the second is released during the iterations. It is interesting to note that during the iterations the program automatically increases the penalty parameter in order to obtain convergence in the dual variables. When the penalty

parameter becomes bigger than a threshold, there is a jump in the value of the displacement of the "released node" from the initial assigned value to a second one very close to the final displacement. In the subsequent iterations, the solution is refined to the required precision. In the graph we also reported the number of Newton's steps preceding the multiplier update. Usually, the rate of convergence was very good, once the program automatically selected "good" values for the penalty parameters (that can be different from node to node).

6. CONCLUSIONS

A generalized complementary energy principle has been used for implementing an algorithm for the analysis of contact problems, which is believed to be particularly convenient for problems concerning no-tension or no-compression materials. Regularization of the governing functional has been achieved by introducing an augmented Lagrangian function, continuous with its second gradient in the neighbourhood of the solution, so that numerical convergence of the algorithm is ensured.

The use of convex potentials of the contact variables in the formulation makes the application of the algorithm to more general constitutive laws of the unilateral constraints very easy, provided they are reversible. Indeed, in the example presented in Section 2, it is only needed to add a further augmented Lagrangian function, and the algorithm would preserve its convergence properties.

REFERENCES

1. M. Cuomo and G. Ventura, An augmented Lagrangian formulation for the analysis of no-tension structures with unilateral supports, In *Contact Mechanics*, (Edited by M. Raous, M. Jean and J.J. Moreau), pp. 247–250, Plenum Press, (1995).
2. M. Cuomo and L. Contrafatto, A variationally consistent incremental principle for the elasto-plastic problem based on complementary energy, In *Computational Plasticity*, (Edited by E. Onate and D.R.J. Owen), pp. 2249–2260, Pineridge Press, (1995).
3. J. Simo and T. Laursen, An augmented Lagrangian treatment of contact problems involving friction, *Computers & Structures* **42** (1), 97–116 (1992).
4. J.H. Heegaard and A. Curnier, An augmented Lagrangian method for discrete large-slip contact problems, *Int. J. Num. Meth. in Engineering* **36**, 569–593 (1993).
5. M. Cuomo and G. Ventura, An effective computational implementation of the no-tension model for masonry structures, In *Computer Methods in Structural Masonry*, (Edited by G.N. Pande and J. Middleton), B.J. International, Swansea (1994).
6. I. Ekeland and R. Temam, *Analyse Convexe et Problèmes Variationnels*, Dunod, Paris, (1974).
7. G. Romano, G. Rosati, F. Marotti de Sciarra and P. Bisegna, A potential theory for monotone multivalued operators, *Quart. Appl. Math.* **LI** (4), 613–631 (1993).
8. G. Romano, G. Rosati and F. Marotti de Sciarra, Variational formulations of non-linear and non-smooth structural problems, *Int. J. Nonlin. Mech.* **28** (2), 195–208 (1992).
9. P.D. Panagiotopoulos, A linear analysis approach to the solution of certain classes of variational inequality problems in structural analysis, *Int. J. Solids Structures* **16**, 991–1005 (1980).
10. A. Klarbring and G. Bjorkman, A mathematical programming approach to contact problems with friction and varying contact surface, *Computers & Structures* **30**, 1185–1198 (1988).
11. A. Klarbring, Contact problems with friction by linear complementarity, In *Proc. of Unilateral Problems in Structural Analysis*, Vol. 2, Springer-Verlag, (1987).
12. A.V. Fiacco and G.P. McCormick, *Nonlinear Programming: Sequential Unconstrained Minimization Techniques*, Wiley, (1968).
13. M. Cuomo, Computational considerations about some classes of penalty formulations for contact problems, In *New Development in Structural Mechanics*, Proceedings of the International Meeting, Catania (1990).
14. J. Simo, P. Wriggers and R. Taylor, A perturbed Lagrangian formulation for the finite element solution of contact problems, *Comp. Meth. Appl. Mech. and Engnr.* **50**, 163–180 (1985).
15. R. Glowinski and P. Le Tallec, *Augmented Lagrangian and Operator-Splitting Methods in Nonlinear Mechanics*, SIAM, Philadelphia, PA, (1989).
16. J.Ph. Bille, S. Cescotto, A.M. Habraken and R. Charlier, Numerical approach of contact using an augmented Lagrangian method, In *Contact Mechanics*, (Edited by R. Raous, M. Jean and J.J. Moreau), pp. 243–246, Plenum Press, (1995).
17. M.R. Hastenes, Muliplier and gradient method, *J. of Optimization Theory and Applications* **4**, 303–320 (1969).

18. M.J.D. Powell, A method for non-linear constraint in optimization problems, In *Optimization*, (Edited by R. Fletcher), pp. 283–298, Academic Press, London, (1969).
19. D.P. Bertsekas, *Constrained Optimization and Lagrange Multiplier Methods*, Academic Press, (1982).
20. J.T. Oden and N. Kikuchi, Finite element methods for constrained problems in elasticity, *Intl. J. Numer. Meth. in Engn.* **18**, 701–725 (1982).
21. J. Haslinger, Approximation of contact problems. Shape optimization in contact problems, In *Nonsmooth Mechanics and Applications*, Springer-Verlag (1988).
22. R.A. Tapia, Diagonalized multiplier methods and quasi-Newton methods for constrained optimization, *J. of Optimization Theory and Applications* **22**, 135–194 (1977).
23. M. Cuomo and G. Ventura, Valutazione dei moltiplicatori nel metodo del Lagrangiano aumentato, *Proceedings of the XII Conference of AIMETA*, Vol. 1, pp. 51–57, Napoli, (1995).